Research Article **CODEN: IJRPJK** **ISSN: 2319 – 9563**

International Journal of Research in Pharmaceutical and Nano Sciences

Journal homepage: **www.ijrpns.com**

SYNTHESIS, CHARACTERIZATION AND CELL UPTAKE OF NANOPARTICLES FOR A NOVEL APPROACH TO RADIONUCLIDE THERAPY: A FEASIBILITY STUDY

Domenica Marabello*[1], Paola Antoniotti[1], Paola Benzi[1], Fabio Beccari[1], Carlo Canepa[1], Alessandro Barge[2], Valentina Boscaro[2], Margherita Gallicchio[2], Elena Peira[2]

[1*]Dipartimento Di Chimica, Universita Degli Studi Di Torino, Torino.
[2]Dipartimento Di Scienzae Tecnologia Del Farmaco, Universita Degli Studi Di Torino, Torino.

ABSTRACT

In this work we report the synthesis of nanoparticles (NPs) of solid crystalline materials with theranostic properties, based on the biocompatible components fructose and $SrCl_2$ or SrI_2. We suitably modified the NPs surface, with simple and fast methods, in order to allow their survival in biological environments. Preliminary viability assay and cell uptake tests were performed on non-tumor and tumor cell lines, hTERT-HME1 and HT-29, respectively. Furthermore, a simple computational tool to evaluate the specific activity of NPs containing ^{89}Sr and ^{131}I required to deliver a pre-determined dose to the cancer tissue was developed, in order to rapidly estimate the amount of NPs to be administered to the patient. The results are discussed in the context of developing novel biocompatible materials for personalized radionuclide therapy.

KEYWORDS

Metal Organic Frameworks, NLO properties, Phospholipidic nanoparticles, Radionuclide therapy, Personalized therapy and Theranostic.

Author for Correspondence:

Domenica Marabello,
Dipartimento Di Chimica,
University of Torino, Torino, Italy.

Email: domenica.marabello@unito.it

INTRODUCTION

In the context of cancer therapy and personalized medicine, a growing interest is now being paid toward theranostic agents, *i.e.* materials bearing at the same time diagnostics and therapy functions[1]. For this purpose, nanoparticles (NPs) are being investigated, because of their potential of being engineered with precise sizes, shapes, composition, and with surface-targeting ligands that allow a specific interaction with target cells[2,3]. The

combination in the same NP of light-based diagnostics and therapy functions have become indispensable tools to address patient-specific characteristics of cancer, claiming an increasing interest in applied research for personalized medicine[4,5].

In the case of cancer, NPs preferentially accumulate in tumors due to the enhanced permeability and retention effect[6]. In fact, nanosystems with long circulation times accumulate preferentially into tumor tissue through a leaky tumor vasculature and are retained in the tumor bed due to reduced lymphatic drainage. This process is known as the enhanced permeability and retention (EPR) effect. Most nano-sized systems accumulate within tumors due to the EPR effect[7] and thus in principle they can improve the performance of radionuclide therapy[8]. The utilization of NPs has a particular advantage, as they are able to achieve a large dispersion within tumor the tissue and closely interact with specific sub cellular structures[9]. In order to be efficiently employed in radionuclide therapy, NPs are required, i) to be rapidly synthetized, ii) rapidly reach their target (tumor cells) and mainly accumulate near or inside it, iii) release sufficient energy to destroy tumor cells, iv) to be easily eliminated body without secondary damage[10,11].

^{89}Sr and ^{131}I are both βemitters, already employed in radionuclide therapy because of their low chemical toxicity and low half-life that reduces post-treatment risks. ^{89}Sr is currently used for treatment of metastases and pain in bone cancer[12,13], because of its ability to substitute the calcium ion in bones and thus acting selectively in these organs. ^{131}I-therapy is a standard ablative therapy for both non-malignant thyroid diseases as well as thyroid cancer, due to its ability to concentrate in this organ[8]. However, though a certain degree of selectivity to the target organ is achieved, both tumor and healthy cells are involved in the irradiation, implicating a not desirable amount of secondary damage to the patient. Thus, it can be useful to encase the radioisotopes into NPs, whose surface can be functionalized in order to drive them exclusively toward tumor cells. At the same time, the concentration of radioisotopes into as small particles can in principle enhance the efficacy of radionuclide therapy.

The aim of this work is to synthetize non-toxic and low-cost Sr/I-based NPs with suitable modified surface for biological employment, in order to develop a new ^{89}Sr- and/or ^{131}I-based radionuclide therapy method.

In our previous works[14-16], we reported on Metal Organic Frameworks (MOFs) obtained by combining fructose with several binary salts MX_2 (M = Ca, Sr; X = Cl, Br, I), that can be utilized as nonlinear optics (NLO) bio-sensors. Among these compounds, we focused our attention to those containing Sr and I, since they can be usefully employed as carriers for ^{89}Sr and ^{131}I.They are $SrCl_2$- and SrI_2-fructose based crystalline compounds, of formula $[Sr(C_6H_{12}O_6)_2\ (H_2O)_2]\ Cl_2{\cdot}H_2O$ (1) and $[Sr(C_6H_{12}O_6)_2]I_2$ (2), respectively. The great advantage of these systems is their biocompatibility, being composed of a sugar and several ions that are known to be metabolized by biological cells. In our previous works, we completely characterized these materials with single crystal X-ray diffraction (Figure No.1) and we discussed their NLO properties for applications as bio-sensor. The purpose of this work is to produce particles of these compounds at nano-scale dimensions for biological applications and to modify their surfacein order to allow their survival in a biological environment. In order to investigate the possible occurrence of structural and functional alterations related to the permanence on NPs in the intracellular milieu, preliminary viability and cell uptake assays were performed on a non-tumor cell line, hTET-HME1, and a tumor cell line, HT-29. Furthermore, the dose absorbed by cancer tissues exposed to ^{89}Sr and ^{131}I enriched NPs was estimated, in the perspective of evaluating the suitable concentration of enriched NPs to administer to the patient. The results are discussed in the context of developing novel biocompatible materials that can be suitably used as carriers of radioisotopes at the sub-cellular level.

MATERIAL AND METHODS

β-D (-) fructose, $SrCl_2 \cdot 6H_2O$, $SrI_2 \cdot 6H_2O$, ethanol, exane and dodecanoyl chloride ≥ 99% were purchased from Sigma-Aldrich. 1, 2-distearoyl-sn-glycero-3-phosphoethanolamine-N-[methoxy (polyethylene glycol)-2000] (mPEG-DSPE) was purchased by Creative PEG Works. All reagents were used as supplied.

Cells. hTERT-HME1 and HT-29 were purchased from American Type Culture Collection (Manassas, VA). hTERT-HME1 were cultured in DMEM-F12 medium, supplemented with 2% fetal bovine serum (FBS), 20ng/mL Epidermal Growth Factor (EGF), 10μg/mL insulin and 100μg/mL hydrocortisone. HT-29 were cultured in RPMI medium supplemented with 10% FBS. All cell culture media were supplemented with 100 units/mL penicillin, 0.1mg/mL streptomycin, 0.25μg/mL amphotericin B and 2mM glutamine.

Synthesis of $Sr(C_6H_{12}O_6)_2$ $(H_2O)_2]$ $Cl_2 \cdot H_2O$ (1) and $Sr(C_6H_{12}O_6)_2]I_2$ (2)

Strontium salts and fructose were dissolved in ethanol at 338 K in the stoichiometric ratio 1:2. After a few minutes the reagents completely dissolved and a faint precipitate was deposited at the bottom of the solution. The precipitate was decanted, washed three times with ethanol, and dried out in an oven at 333 K.

Synthesis of nanoparticles (NPs)

The precipitates were ground in a planetary ball mill (Retsch PM 100) equipped with steel jars with volume of 50mL and balls with diameter of 2mm. The grinding parameters were: i) 200 rpm, 2 minute pause for each 5 minutes of grinding and ii) 300rpm, 2 minutes pause for each 8 minutes of grinding. 20mg of ground powder were mixed with 0.3mg of fluorescein and suspended through sonication in 2mL of hexane. The suspension was transferred into an agate mortar and ground with 10μL of dodecanoyl chloride. The suspension was dried in an oven at 333 K. To enclose NPs in a lipid shell, 6 mg of the previous product were mixed with 0.6 mg of mPEG-DSPE and 2mL of hexane. After 30 minutes of sonication the suspension was quickly dried in the oven at 333K. Prior to the biological tests the powder obtained was suspended in water and sonicated for30 minutes.

NPs characterization

X-ray powder diffraction. XRPD patterns were collected at room temperature using an Oxford Diffraction Gemini R Ultra diffractometer. Data were collected with mirror monochromatized Cu-Kα radiation (λ=1.5418 Å): maximum resolution 1.4 Å, exposure time 30 s and data collection and integration with Crys Alis Pro software[17].

Size measurement. The NP average diameters and polydispersity index (PDI) were characterized by Laser Light Scattering technique (LLS), performed using a 90Plus Nanoparticle Size Analyzer equipped with a Peltier temperature control system (Brookhaven Instruments Corp., Holtsville, NY). The particle size measurements and distribution were carried out at 25°C, at a fixed 90° angle and a wavelength of 675nm.

To maximize the accuracy of the measurement, the modified NPs were diluted before the LLS analysis by using 4mL of Milli Q water and sonicated for 30 minutes. As a measure of an acceptable sample concentration, we followed the recommendation of the LLS equipment manufacturer that the signal intensity measured by the instrument lie between 100 and 250 kilo counts per second (kcps).

Cells and viability assay

Viability assay. Cells were seeded in complete medium (100μL) at an appropriate density (1000-10000 cells/well), in 96-well plastic culture plates in triplicate. The following day, after serial dilutions in medium, 100μL of modified NP, fructose or strontium chloride, in serum-free medium, were added to the cells using a multichannel pipette; medium-only containing wells were used as controls. Plates were incubated at 37 C in 5% CO_2 for different times (1, 2 or 5 days), after which the cell viability was assessed using ATP content and the Cell Titer-Glo® Luminescent Cell Viability Assay (Promega, Italia Srl, Milano, Italy). All luminescence measurements (indicated as relative light units), were recorded on a Victor X4 multimode plate reader (Perkin-Elmer, Waltham, MA, USA).

Cell uptake. 150.000 cells were seeded in complete medium (250μL) in each well of a 24-well plastic culture plates, in triplicate. The cells were incubated for 24 h and subsequently treated with different concentrations of NPs loaded with fluorescein for 3 or 24 h; medium-only containing wells were used as controls. Supernatants were collected and cells were washed twice with phosphate buffer saline and lysed using Alpha Sure Fire Ultra Lysis Buffer (5X) (Perkin Elmer). Both the supernatant and the intracellular fluorescence were recorded using an Ensight multimode plate reader (Perkin-Elmer, Waltham, MA, USA)[18].

RESULTS AND DISCUSSION

Compounds 1 and 2 were rapidly synthetized using the direct reaction of salts and fructose in ethanol, that led to the formation of a faint white precipitate. The main disadvantage for biological application of this kind of materials is their high solubility in water. To avoid their dissolution, the NPs were reacted with dodecanoyl chloride, to saturate the -OH groups on the surface and reduce their polarity. Ester bonds are formed on the surface of the NPs, and the long hydrophobic chains make the NPs completely waterproof, as evidenced in Figure No.2, where a drop of water mixed with the modified powder was observed on an optical stereo-microscope (drop on the left).

However, for biological applications the NPs should be able to diffuse in a water medium. For this purpose, we created a hydrophilic shell of mPEG-DSPE that increases their biocompatibility. The NPs enveloped with mPEG-DSPE become completely hydrophilic, as shown by their diffusion into the drop of water shown on the right side of Figure No.2. The complete process of chemical modification of NPs surface is schematized in Figure No.3.

In Figure No.4 reports the XRPD patterns collected for compounds 1 (ground for 90 min at 200rmp) and 2 (ground for 90 min at 300rmp), after reaction with dodecanoyl chloride and the subsequent covering with mPEG-DSPE: the comparison of the experimental XRPD patterns to the calculated from the single crystal X-ray structures of the two compounds shows that the crystalline core maintained its integrity. Thus, the intact crystalline frameworks of the compounds preserve their NLO property, that can be exploited for the bio-sensing of NPs inside the cells.

To obtain NPs of suitable dimensions for biological applications, each dried precipitate was ground on a planetary ball mill, exploiting its high fragility. The products are stable in a wide range of temperatures, up to 323 K. Since they quickly degrade under an electron beam, it was not possible to characterize the primary particle sizes of NPs with SEM or TEM microscopes. Thus, the LLS technique was used to determine the particle size distribution in the sub-micrometric range. Table No.1 reports the mean diameter and standard error of the particles modified with dodecanoyl chloride and covered with mPEG-DSPE, obtained with different grinding parameters.

As shown in Table No.1, for both compounds the mean modified NPs size decreases with grinding time; moreover, compound 2 needs enhanced grinding energy with respect to compound 1 to obtain the same dimension.

In conclusion, by conveniently selecting the grinding parameters, we can regulate the dimension of NPs to the biological and therapy requirements.

Evaluation of the dose absorbed by a tissue exposed to enriched nanoparticles of compound1 (^{89}Sr(fructose)$_2$ Cl$_2$·H$_2$O) and compound 2 (^{89}Sr (fructose)$_2$I$_2$ and Sr (fructose)$_2$^{131}I$_2$)

The compounds presented in this paper, once enriched in^{89}Sr or ^{131}I, could be of interest for applications in biomedicine and in radiotherapy. Radioactive nuclides of both the cation and the anion can be obtained by nuclear fission, and the two inorganic compounds strontium chloride and sodium iodide are currently available in forms suitable for applications in radiotherapy. ^{89}Sr, is aβ emitter with a half-life of 50.57 d used in the form of chloride for metastasized bone cancer; ^{131}I is also aβ emitter with a half-life of 8.0252 d, used in the form of sodium iodide for hyperthyroidism and carcinoma of the thyroid. Considering that

strontium chloride and sodium iodide do not exhibit any selectivity towards tumor cells while nanoparticles can be functionalized to selectively bind to tumor cells, we have computed the dose absorbed by a tissue exposed to nanoparticles of $^{89}Sr(fructose)_2I_2$ and $Sr(fructose)_2{}^{131}I_2$ containing a number density ρ of the relevant radionuclide, assuming the radius of particles to be $r_c = 0.10\ \mu m$.

The average energy of the β^-radiation emitted by^{89}Sr and ^{131}I is 0.58 MeV ($E_\beta = 9.29 \times 10^{-14} J$) and 0.19 MeV ($E_\beta = 3.07 \times 10^{-14} J$), respectively.

Based on the ranges computed in the continuous slowing down approximation of 2.3 mm (for^{89}Sr) and 0.45mm (for^{131}I), we can safely assume that the tumor size is about one order of magnitude larger.

That leads to the assumption that in the tissue the distance between particles, each of volume v_c, is smaller than the average range of the β radiation, and all theβ energy would be absorbed by the tumor tissue. Consequently, to deliver a predetermined dose to a tumor mass that contains within itself a number density of particles $\mathbf{P}$ and it is made of cells of volume v_{cell}, we need the specific value of the atomic number density $\hat{\rho}$ (atoms m^{-3}) of the radionuclide (^{89}Sr or^{131}I) in the tissue, given by

$$\hat{\rho} = \mathbf{P} v_{cell} \rho \frac{v_c}{v_{cell}}$$

$$= \mathbf{P} v_{cell} \rho \left(\frac{r_c}{r_{cell}}\right)^3 \quad (1)$$

The required density $\hat{\rho}$ would be attained by either scaling the radionuclide atomic density in the particle (ρ) or the number of particles in the cell ($\mathbf{P} v_{cell}$). For example, the commercial water solution of$^{89}SrCl_2$ contains, on average, 16.75 mg of strontium chloride per mL with the activity of 37MBq mL^{-1}, corresponding to the average specific activity 4.565 MBq mg^{-1}. Particles of$^{89}Sr(fructose)_2I_2$ synthesized from this commercial solution would have a fixed atomic density of^{89}Sr, and the number density 1.49×10^{22} ^{89}Sr atoms per cubic meter can be calculated from the relation $a = \lambda N$ (a represents the activity and λ is the ^{89}Sr decay constant) and the $^{89}Sr(fructose)_2I_2$ mass density of 2.307×10^3 kg m^{-3}. With this value we evaluate $\hat{\rho}$ and the energy per unit mass absorbed by the tissue

$$\hat{E}_\beta = \hat{\rho} \frac{E_\beta}{\rho_w} \quad (2)$$

The integrated dose thus is

$$D = \hat{E}_\beta \left(1 - e^{-\lambda t}\right) \quad (3)$$

To deliver a predetermined dose D_{min} to the tumor mass, we would need to scale either the value of $\mathbf{P} v_{cell}$ or ρ to satisfy the equality$D = D_{min}$.

In the case of $^{89}Sr(fructose)_2I_2$, we would need $\mathbf{P} v_{cell} = 0.25$ for D_{min}= 1 Gy (Gy = Jkg^{-1}). Thus a tumor with cell radius $r_{cell} = 7\mu m$, as in glioblastoma cell lines[19], treated with these particles would be delivered a dose of 1 Gy by a particle density $\mathbf{P} v_{cell} \approx 0.25$, i.e. about 1 particle in four cells. If the resulting distribution of particles had a lower density, the only way to reach the limit value of 1 Gy would be to resort to a starting material with a higher specific activity.

On the other hand, since commercial $Na^{131}I$ is isotopic ally pure, particles of $Sr(fructose)_2{}^{131}I_2$ derived by the commercial salt would afford the high atomic density of^{131}I ρ= 3.95×10^{27} m^{-3}. To deliver 1 Gy, we would thus need to scale downρ by a factor 2.85×10^{-6} for the particle density in the case $\mathbf{P} v_{cell} = 1$, i.e. only one particle per cell.

Table No.5 reports the calculated values of ρ and $\hat{\rho}$ for D_{min} = 1Gy and $Sr(fructose)_2I_2$ labeled with ^{89}Sr or ^{131}I from $^{89}SrCl_2$ or $Na^{131}I$ as starting reagents, respectively.

In order to be able to calculate the required initial activity for each specific therapy, we need the initial activity per unit of irradiated tissue volume, as given by

$$\frac{a_0}{v_t} = \lambda \hat{\rho} \quad (4)$$

Values of a_0/v_t ($Bq\ m^{-3}$) are also reported in Table No.2 for the compounds studied. For a tumor with radius 1 cm ($m \cong 0.005$ kg) and the fraction $f_{^{89}Sr}$=

$7.57 \times 10^{-6}$of radionuclide ^{89}Sr in the starting compound, $a_0 = 7.16 \times 10^3$Bq, the corresponding amount of crystal ($^{89}Sr(fructose)_2I_2$ or $^{89}Sr(fructose)_2Cl_2 \cdot 3H_2O$) is

$$\frac{\hat{\rho} v_t}{f_{^{89}Sr} N_A} = 9.89 \times 10^{-9} \text{mol} \quad (5)$$

(Corresponding to 6.94μg and 5.67μg, respectively).

The two β^- emitters have thus complementary features; ^{89}Sr exhibits a long half-life that would ease both the formation and the functionalization of the particles at the expense of a dose somehow limited by the factor $\mathbf{P}v_{cell}$.

On the other hand, ^{131}I makes a virtually unlimited dose readily available (in fact, it would have to be diluted to deliver a dose of 1 Gy with $Sr(fructose)_2{}^{131}I_2$ particles), but it has a relatively short half life that calls for a fast preparation and use of the particles. From the above considerations, it should be possible to tune the therapeutic properties of nanoparticles by calibration of the amount of ^{89}Sr and/or ^{131}I, thus allowing the custom-tailoring of the therapy to the patient.

In conclusion, equations (1) trough (5) can allow the custom-tailoring of the therapy to the patient through the estimate of the amount of enriched NPs to be administered to the patient once the bio-distribution, clearance, and specific uptake are known.

Viability assay

To evaluate the effect of the NPs on cell viability, we treated hTERT-HME1 and HT-29 cell lines with five different modified NPs concentrations, in the range 0.25 – 0.000025mg/mL, for 1, 2 and 5 days. Subsequently, the cell viability was determined using the luminescent detection of cellular ATP content; each point was performed in triplicate and at least three times. As shown in Figure No.5, modified NPs of both compounds1 and 2 were not able to significantly influence cell viability of both cell lines at day 1 and 2. After 5 days the hTERT-HME1 cell line showed sensitivity to compound 1 at the lowest concentration, even though with a high standard deviation. Instead, compound 2 reduced hTERT-HME1 cell viability in a dose-dependent manner. HT-29 viability was reduced by about 70% and 50% only at the highest concentration of modified NPs of compounds 1 and 2, respectively. We treated the hTERT-HME1 and HT-29 cell lines also with solutions of fructose, strontium chloride, and strontium iodide at the same concentration of the modified NPs and that did not alter the cell viability (see Figure No.6). We conclude thus that the viability is influenced only by the presence of the NPs themselves rather than their chemical composition, as expected.

Cell uptake

The intracellular uptake of modified NPs was evaluated by loading fluorescein into the NPs and measuring the intracellular fluorescence intensity. As shown in Figure No.7, the fluorescence intensity was greater when cells were incubated with the highest modified NPs concentration, both for compounds 1 and 2. Furthermore, it increased as a function of the incubation time and it was greater in hTERT-HME1 than in HT-29.

Regarding modified NPs of compound 2, the intensity of the intracellular fluorescence increased in a dose-dependent manner after 3 h of treatment in both cell lines, while there was no dose-dependent correlation after 24 h.

Table No.1: Mean diameter± standard error and PDI of the particles obtained by grinding the powders on a planetary ball mill, with different revolutions per minute (rpm) and grinding times for compounds 1 and 2

S.No	Grinding time	rpm	Mean diameter nm ± s.e. (PDI)
Compound 1			
1	33 min	200	275.4 ± 27.3 (0.305)
2	44 min	200	236.9 ± 19.6 (0.246)
3	55 min	200	149.0 ± 11.9 (0.232)
4	66 min	200	134.9 ± 8.1 (0.227)
Compound 2			
5	33 min	200	467.2 ± 40.0 (0.005)
6	44 min	200	432.7 ± 44.0 (0.005)
7	55 min	200	383.8 ± 74.0 (0.164)
8	66 min	200	372.5 ± 72.3 (0.320)
9	74 min	300	333.4 ± 6.0 (0.280)
10	98 min	300	257.0 ± 3.2 (0.296)

Table No.2: Number density of the radionuclide in the particles (ρ/m^{-3}) and in tissue ($\hat{\rho}/\mathrm{m}^{-3}$) for the specified average number of particles per cell. The isotopic dilution factor δ and total activity per unit of irradiated volume are also reported for a delivered maximum dose $\bar{E}_{\beta} = 1$ Gy. The cell radius is assumed to be $7\,\mu$m, as in glioblastoma cell lines

S.No	*Crystal*	ρ/m^{-3}	$\hat{\rho}/\mathrm{m}^{-3}$	$\mathrm{P}v_{cell}$	δ	$(a_0/v_c)/\mathrm{Bqm}^{-3}$
1	^{89}Sr(fructose)$_2$I$_2$	1.49×10^{22}	1.08×10^{16}	0.25	1	1.71×10^{9}
2	^{89}Sr(fructose)$_2$Cl$_2\cdot 3$H$_2$O	1.38×10^{22}	1.08×10^{16}	0.27	1	1.71×10^{9}
3	Sr(fructose)$_2{}^{131}$I$_2$	1.13×10^{22}	3.29×10^{16}	1	2.85×10^{-6}	3.28×10^{10}

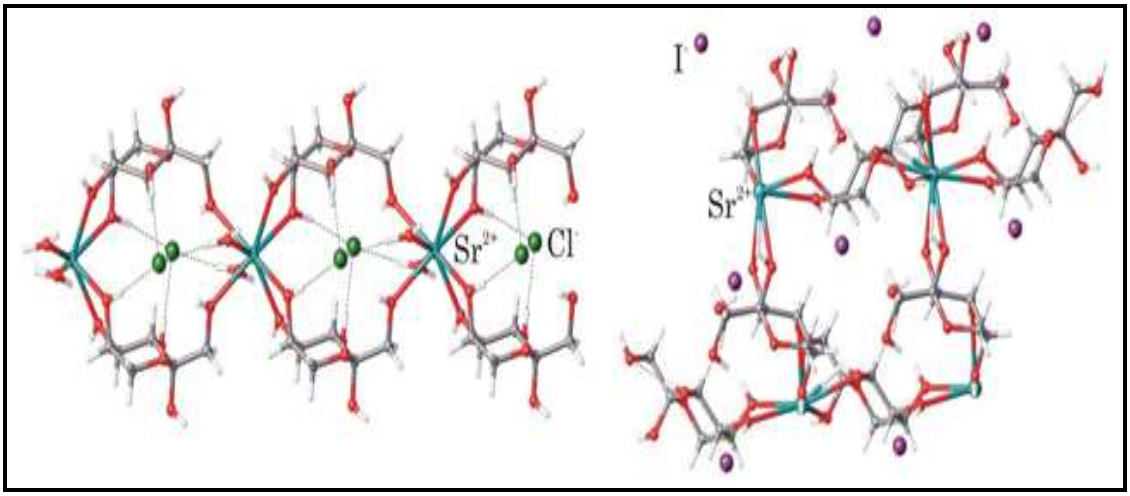

Figure No.1: Crystal structures of compounds 1 (left) and 2 (right). The complete characterization of these materials are reported in references 14 and 16

Figure No.2: Observation on an optical stereo-microscope of a drop of water with the powder of compound 1 reacted with dodecanoyl chloride (left) and with m-PEG (right)

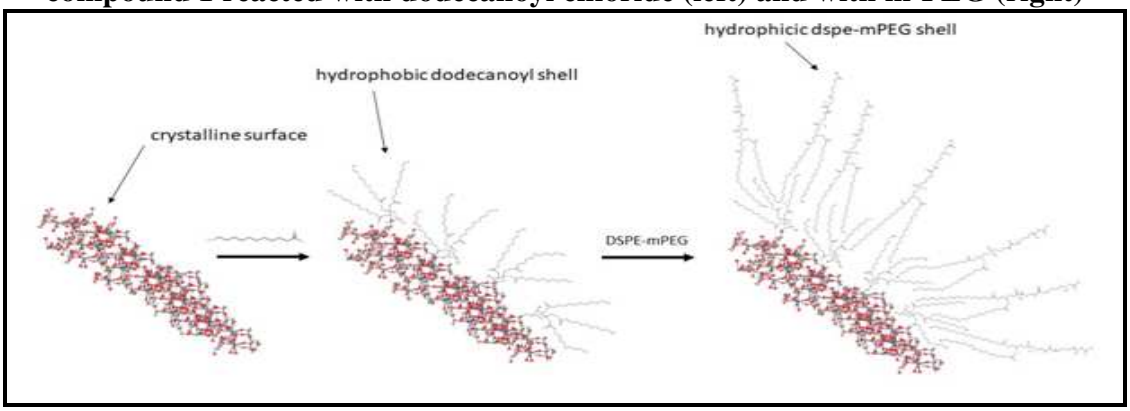

Figure No.3: Chemical surface modification steps aimed to avoid the dissolution of nanoparticles and at the same time allow suspension in a biological medium

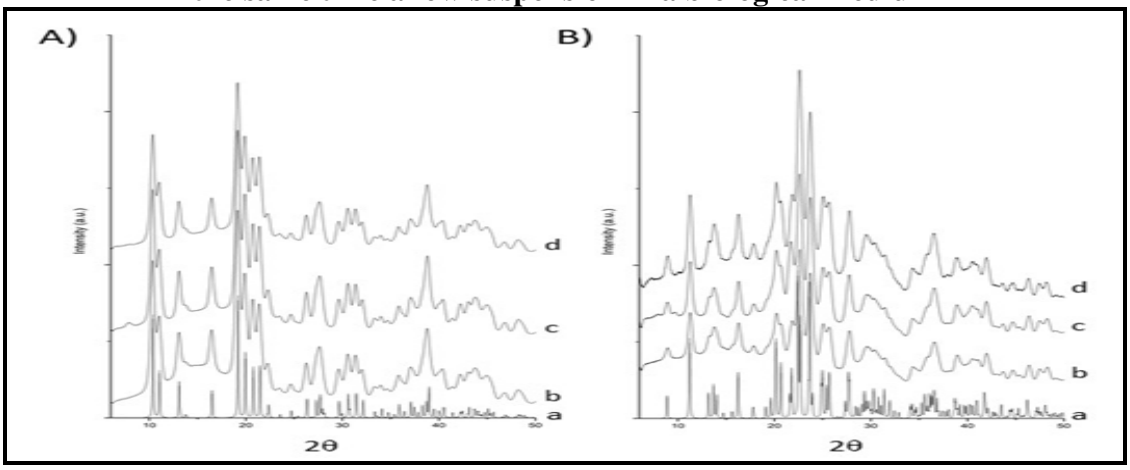

Figure No.4: XRPD patterns collected for compounds 1 (A) and 2 (B) before treatment (b), after reaction with dodecanoyl chloride (c), and after the subsequent covering with mPEG-DSPE (d), compared to the respective XRPD patterns calculated from the XRD structures (a)

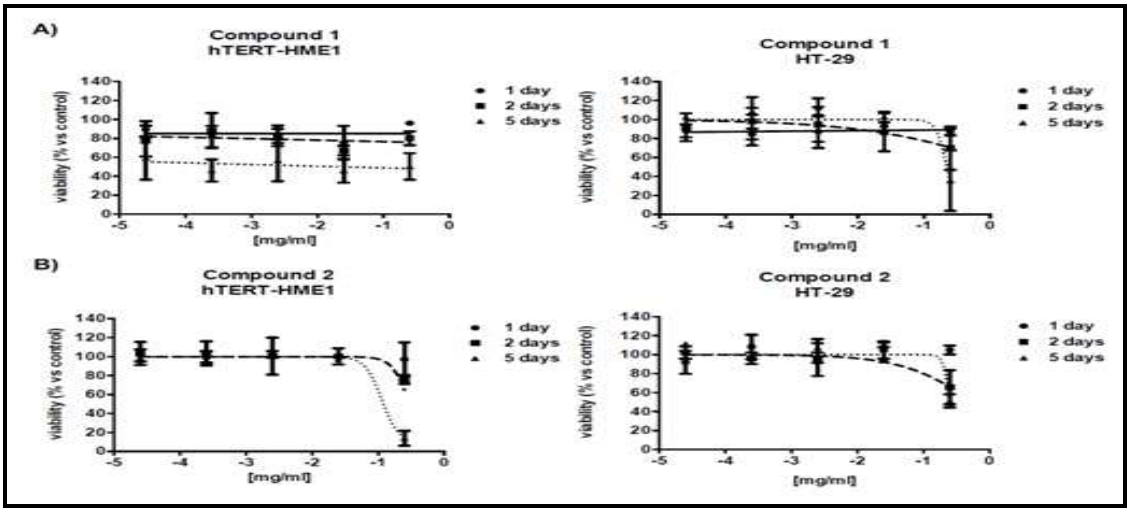

Figure No.5: Antiproliferative activity of nanoparticles of compounds 1 (A) and 2 (B) in hTERT-HME1 and HT-29

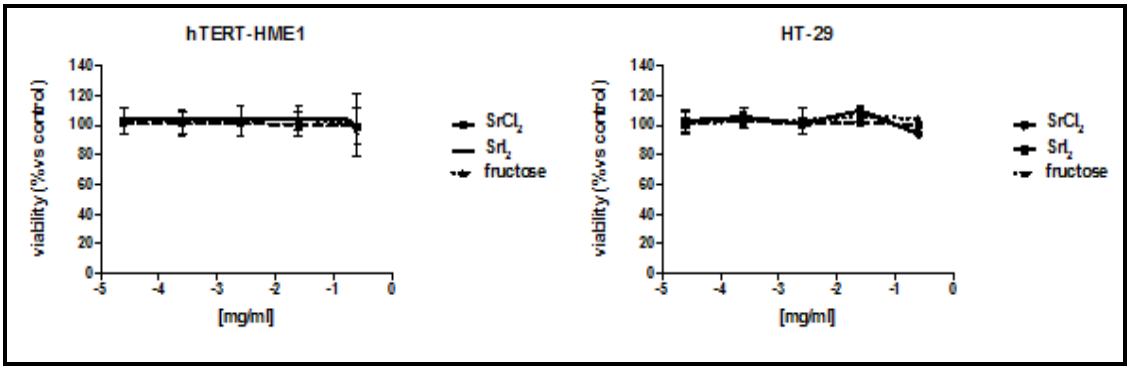

Figure No.6: Antiproliferative activity of solutions of fructose, strontium chloride, and strontium iodide in hTERT-HME1 and HT-29

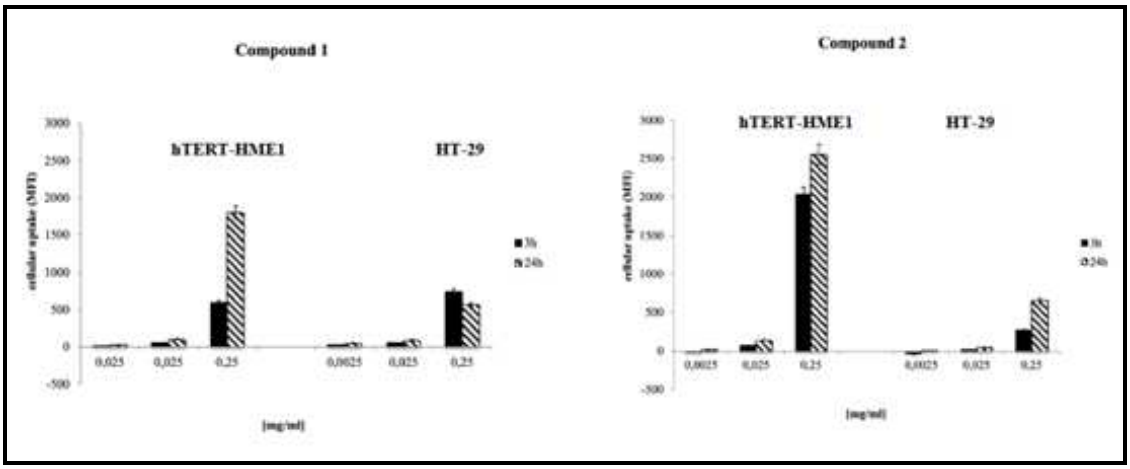

Figure No.7: Cellular uptake of nanoparticles of compounds 1 and 2 in hTERT-HME1 and HT-29 cells after 3 and 24 h. Fluorescein was used as a fluorescent dye and the amount of fluorescence intensity in the cells was interpreted in terms of cellular internalization capacity. Data are expressed as means ± S.D. of at least 3 different experiments, run in triplicate

CONCLUSION

In this work we optimized the synthesis and covering of NPs of compounds 1 and 2 in view of their use as carriers of ^{89}Sr and ^{131}I into tumor cells. The NPs are rapidly and easily synthetized and their size can be regulated simply by modulating the grinding energy. The chemical modification of the NPs surface, in order to allow their dispersion in a biological medium, is also simple and fast, this being a great advantage for radionuclide therapy applications, since both radio-isotopes have a relatively short half-life. The modified NPs were shown to survive for days in a biological medium and internalize into hTERT-HME1 and HT-29 cells. The viability of cell lines utilized is influenced by the presence of the NPs themselves rather than their chemical composition. The NPs formulation could be useful to concentrate the effect of ^{89}Sr and ^{131}I in a specific tissue, allowing a selective activity of the activated compounds. The evaluation of the dose absorbed from a tissue exposed to NPs of $^{89}Sr(fructose)_2Cl_2 \cdot H_2O$, $^{89}Sr(fructose)_2I_2$, and Sr $(fructose)_2{}^{131}I_2$ suggests that these compounds could be successfully employed in radionuclide therapy. The two β^- emitters show complementary features: ^{89}Sr would ease both the synthesis and the functionalization of the particles at the expense of a dose somehow limited; ^{131}I, on the other hand, would need a fast preparation and use of the particles, but it makes a virtually unlimited dose readily available. From the above considerations, it follows that the calibration of the amount of ^{89}Sr and/or ^{131}I inside the NPs, should enable us to deliver a specified dose to each patient, thus allowing the custom-tailoring of the beta therapy. Moreover, we developed a tool to rapidly estimate the amount of labeled NPs to be administered to the patient, as a function of the required dose to treat a tumor mass of a specified size. The great advantage of encapsulating the enriched isotopes into NPs are: i) the concentration of the enriched isotopes into a small volume, that can locally enhance the dose administered and reduce side effects to the patient; ii) the possibility to easily functionalize the NPs surface depending on the target tumor cells. Thus, in principle, the same isotope can be used for a wide range of tumors by simply varying the functionalization of the surface. This will be the aim of our further work.

ACKNOWLEDGEMENT

Financial support from MIUR (Ministerodell' Istruzione, Dell' Universitae Della Ricerca) and Fondazione CRT is acknowledged.

CONFLICT OF INTEREST

We declare that we have no conflict of interest.

REFERENCES

1. Jeong H J, Lee B, Ahn B C, Kang K W. Development of Drugs and Technology for Radiation Theragnosis, *Nucl. Eng. And Techn*, 48(3), 2016, 597-607.
2. Ferrari M. Cancer nanotechnology: opportunities and challenges, *Nat. Rev. Cancer,* 5(3), 2005, 161-171.
3. Sahoo S K, Parveen S, Panda J J. The present and future of nanotechnology in human health care, *Nanomedicine,* 3(1), 2007, 20-31.
4. Ryu J H, Lee S, Son S, Kim S H, Leary J, Choi K, Kwon I C. Theranostic nanoparticles for future personalized medicine, *J. Control. Release,* 190, 2014, 477-484.
5. Ting G, Chang C H, Wang H E, Lee T W. Nanotargeted radionuclides for cancer nuclear Imaging and internal theraphy, *J. Biomed. Biotechnol,* 2010, Article ID 953537, 2010, 1-17.
6. Noguchi Y, Wu J, Duncan R, Strohalm J, Ulbrich K, Akaike T, Maeda H. Early Phase Tumor Accumulation of Macromolecules: A Great Difference in Clearance Rate between Tumor and Normal Tissues, *Jpn. J. Cancer Res,* 89(3), 1998, 307-314.
7. Lammers T, Kiessling F, Hennink W E, Storm G. Drug targeting to tumors: principles, pitfalls and (pre-) clinical

progress, *J. Control. Release,* 161(2), 2012, 175-187.
8. Sheets N C, Wang A. Radioisotopes and Nanomedicine, *In: Singh P N, editor, Radioisotopes - Applications in Bio-Medical Science, Rijeka: In Tech,* 2011, 47-66.
9. Maggiorella L, Barouch G, Devaux C, Pottier A, Deutsch E, Bourhis J, Borghi E, Levy L. Nanoscale radiotherapy with hafnium oxide nanoparticles, *Future Oncol,* 8(9), 2012, 1167-1181.
10. Kwatra D, Venugopal A, Anant S. Nanoparticles in radiation therapy: a summary of various approaches to enhance radio sensitization in cancer, *Transl. Cancer Res,* 2(4), 2013, 330-342.
11. Zhang L, Chen H., Wang L, Liu T, Yeh J, Lu G, Yang L, Mao H. Delivery of therapeutic radioisotopes using nanoparticle platforms: potential benefit in systemic radiation therapy, *Nanotechnol. Sci. Appl,* 3(1), 2010, 159-170.
12. Yaneva M P, Semerdjieva M, Radev L R, Ivanova E K, Geiman M, Vlaikova M I, Mihova L S. Radionuclide therapy of cancer patients with bone metastases, *Folia Med. (Plovdiv),* 47(3-4), 2005, 63-69.
13. Nightengale B, Brune M, Blizzard S P, Ashley-Johnson M, Slan S. Strontium chloride Sr-89 for treating pain from metastatic bone disease, *Am. J. Health Syst. Pharm,* 52(20), 1995, 2189-2195.
14. Marabello D, Antoniotti P, Benzi P, Canepa C, Diana E, Operti L, Mortati L, Sassi M P. Non-linear optical properties of β-D-fructopyranose calcium chloride MOFs: an experimental and theoretical approach, *J. Mater. Sci,* 50(12), 2015, 4330-4341.
15. Marabello D, Antoniotti P, Benzi P, Canepa C, Mortati L, Sassi M P. Synthesis, structure and non-linear optical properties of new isostructural β-D-fructopyranose alkaline halide metal-organic frameworks: a theoretical and an experimental study, *Acta Cryst,* B73(4), 2017, 737-743.
16. Marabello D, Antoniotti P, Benzi P, Cariati E, Lo Presti L, Canepa C. Developing new SrI_2 and β-D-fructopyranose-based metal-organic frame works with nonlinear optical properties, *Acta Cryst,* B75(2), 2019, 210-218.
17. Crys Alis Pro, *Agilent Technologies,* Version 1.171.37.31 (release 14-01-2014 Crys Alis 171. NET, compiled Jan 14 2014, 18:38:05.
18. Wang X B, Zhou H Y. Molecularly targeted gemcitabine-loaded nanoparticulate system towards the treatment of EGFR over expressing lung cancer, *Biomedicine and Pharmacotherapy,* 70, 2015, 123-128.
19. Memmel S, Sukhorukov V L, Horing M, Westerling K, Fiedler V, Katzer A, Krohne G, Flentje M, Djuzenova C S. Cell surface area and membrane folding in glioblastoma cell lines differing in PTEN and p53 status, *PLOS ONE,* 9(1), 2014, e87052.

Please cite this article in press as: Domenica Marabello *et al.* Synthesis, characterization and cell uptake of nanoparticles for a novel approach to radionuclide therapy: a feasibility study, *International Journal of Research in Pharmaceutical and Nano Sciences,* 8(5), 2019, 229-240.